International Journal of Heat and Fluid Flow 29 (2008) 1577–1585

Contents lists available at ScienceDirect

International Journal of Heat and Fluid Flow

journal homepage: www.elsevier.com/locate/ijhff

Nanofluid boiling: The effect of surface wettability

Johnathan S. Coursey, Jungho Kim *

Department of Mechanical Engineering, University of Maryland, College Park, MD 20742, United States

ARTICLE INFO

Article history:
Received 6 November 2007
Received in revised form 6 July 2008
Accepted 30 July 2008
Available online 11 September 2008

Keywords:
Critical heat flux
Boiling
Heat transfer
Contact angle
Nanofluids
Surface energy

ABSTRACT

Nanofluid boiling has shown potential to increase boiling heat transfer, but the mechanisms responsible are poorly understood. One likely mechanism for nanofluid enhancement is an improvement in surface wettability. This study is targeted towards investigating whether or not nanofluids improve the critical heat flux (CHF) by altering the surface energy as has been observed for pure fluids. The surface of a heater was systematically altered by oxidizing its surface to varying degrees or by depositing metal onto the surface, and the surface energy was characterized by measuring the advancing three-phase contact angle. Boiling curves on these surfaces were measured for pure fluids and for water and ethanol based nanofluids with aluminum oxide nanoparticle concentrations from 0.001 g/L to 10 g/L. Dilute suspensions of nanoparticles were found to degrade or have no effect on the boiling performance. Greater concentrations ($\geqslant$0.5 g/L) led to modest (up to ~37%) increase in the CHF. Poorly wetting systems (e.g. water on polished copper) could be enhanced by the addition of nanoparticles, whereas better wetting systems (e.g. ethanol on glass) showed no improvement or a larger degradation. Furthermore, the addition of nanoparticles to water was found to improve wetting, but only when the surface was fouled by the particles. Interestingly, similar CHF enhancement was achieved without nanofluids using an oxidized surface, which was easily wetted with pure fluids. In fact, surface treatment alone resulted in similar CHF enhancement but at ~20 °C lower wall superheat than when using nanofluids.

1. Introduction

Boiling heat transfer continues to be a subject of ongoing research because of its potential to remove large amounts of heat at low temperature difference and a lack of validated models. While boiling has been studied for many years, popular models such as the hydrodynamic instability model (Zuber, 1959), the bubble-packing model (Rohsenow and Griffith, 1956), and the macrolayer model (Haramura and Katto, 1983) neglect many factors that have been shown to affect performance such as gravity, surface wettability and finish, heater dimensions, and heater thermal properties among others. A lack of understanding of the underlying mechanisms presents a significant challenge to efforts aimed at enhancing heat transfer. Furthermore, the lack of verified boiling models presents a specific challenge to the interpretation of the numerous conflicting nanofluid boiling studies reported to date.

Nanofluid boiling has shown promise at least as early as 1984, when Yang and Maa (1984) demonstrated that nanoscale alumina particles (50, 300, and 1000 nm) in water with concentrations of 0.1 and 0.5 wt% could significantly lower the superheat required for a given heat flux. The smallest particles yielded the greatest improvement at 0.1 wt%, while all particle sizes performed equally at 0.5 wt%. The only possible mechanism for enhancement cited though was disturbance of the thermal boundary layer by the motion of the particles.

More recent studies on nanofluid boiling have yielded contradictory results. Das et al. (2003) studied boiling of alumina–water nanofluids with concentrations of 0.1–4 vol.% and found the boiling curve shifted to the right as the nanoparticle concentration was increased (i.e., higher wall temperature for the same heat flux). Bang and Chang (2005) also observed degradation of the heat transfer coefficient in the natural convection and nucleate boiling regimes with alumina–water nanofluids, but CHF was enhanced up to 51%. Both groups attributed the performance degradation in nucleate boiling to deposition of the nanoparticles onto the surface–particle deposition altered the nucleation site density as the surface was smoothed (at least locally), and fouling resulted in poor conduction heat transfer at the surface. Their work was contradicted by Wen and Ding (2005) who used alumina/water nanofluids and observed up to 40% enhancement in nucleate boiling. They attributed the enhancement to the stability of their nanofluids, which did not deposit on the surface.

A group at University of Texas, Arlington (You et al., 2003; Kim et al., 2004; Moreno et al., 2005) used water with various Al_2O_3 particle loadings in a flat plate nucleate pool boiling system. They found little to no change in the heat transfer coefficient but dramatic (up to ~200%) improvement in CHF. Moreno et al. (2005)

* Corresponding author. Tel.: +1 301 405 5437; fax: +1 301 314 9477.
E-mail address: kimjh@umd.edu (J. Kim).

0142-727X/$ - see front matter © 2008 Elsevier Inc. All rights reserved.
doi:10.1016/j.ijheatfluidflow.2008.07.004

Nomenclature

c	concentration (g/L)
q''	heat flux (W/cm^2)
ΔT_{sat}	surface temperature – saturation temperature (K)
y	mass fraction
Greek letters	
θ	advancing contact angle (°)
ρ	density (kg/m^3)
ϕ	volume fraction
Subscripts	
mix	mixture
post	after boiling experiment
prior	before boiling experiment
pure liquid	pure water or ethanol

also used ZnO/water and Al_2O_3/water + ethylene glycol nanofluids. All were found to increase CHF, but high concentrations sometimes resulted in nucleate boiling degradation.

Vassalo et al. (2004) studied pool boiling with 0.5 vol.% micro and nano-solutions. They used 15 nm, 50 nm, and 3 μm silica particles in water. All suspensions were observed to increase CHF by ~60%, but the nucleate boiling regime was unaffected. However, nanofluids had the interesting effect of allowing the wire to continue into transition and film boiling modes. The pure fluid and micro-suspension resulted in wire failure immediately following CHF, while nanofluids resulted in heat fluxes almost 3 times that of pure water, albeit at 1000 °C. The authors noted that this may be due to silica coating the wire.

Milanova and Kumar (2005) observed CHF three times that of the base fluid in a silica nanosuspension depending on the particle size and pH level. Higher pH levels (up to 12.3) were observed to increase CHF while acidic solutions lowered CHF. Relatively little influence on the nucleate boiling regime was seen.

Park et al. (2004) investigated direct quenching of a 10 mm diameter stainless steel sphere in pure water and alumina nanofluids. With initial temperatures of 1000–1400 K and volume concentrations from 5% to 20%, they found that film boiling heat transfer coefficients were consistently lower with nanofluids than pure water. They found that differences in film boiling heat transfer became larger as the subcooling decreased suggesting that the presence of nanoparticles may enhance vapor generation. They further observed markedly different quenching behavior when an unwashed (nanoparticle coated) sphere was used. The unwashed sphere quenched much more rapidly suggesting that nanoparticle deposits prevent the formation of a stable vapor film.

Xue et al. (2006) used carbon nanotubes/water in a closed loop thermospyhon and found that the suspension decreased boiling performance and increased the total thermal resistance of the system. Xue et al. measured the contact angle of sessile drops. Interestingly, the nanofluids had much lower contact angles. Lower contact angle should improve boiling heat transfer (Liaw and Dhir, 1989; Kandlikar, 2001), but this decreased contact angle was accompanied by an increase in contact line hysteresis and greater susceptibility to surface imperfections (i.e., contact line pinning).

Narayan et al. (2007) explored the role of nanoparticle concentration and surface roughness on nucleate boiling heat transfer. Nanofluids increased the heat transfer on the roughest surface used (average roughness R_a = 524 nm) at all concentrations. The heat transfer increased on the heater with R_a = 98 nm up to 0.5 wt% concentration, but deteriorated above that. The smoothest heater (R_a = 48 nm) experienced deterioration in heat transfer with increasing concentration. They concluded that the ratio of the average surface roughness to the average particle size governs whether or not enhancement or deterioration occurs.

Shi et al. (2007) studied boiling of nanofluids on a horizontal plate using Fe–water and Al_2O_3–water suspensions. They observed larger enhancement for the higher conductivity Fe–water solution. It was suggested that the effect of nanofluids suspensions can be enhanced or degraded depending on the interplay between enhanced thermal conductivity and filling of cavities by the particles.

A group at MIT (Kim et al., 2006a; Kim et al., 2007b) measured up to 80% enhancement in CHF using water based nanofluids. They also found that "nano-particle fouled" surfaces significantly improved wettability as measured by a reduction in static contact angle. They suggested that the buildup of a porous layer of nanoparticles on the heated surface during boiling improved surface wettability and promoted liquid rewetting and could explain the enhancement in CHF observed by numerous researchers.

Surface modification was studied by the Pohang University (Korea) group of (Kim et al., 2006b; Kim et al., 2007a) during their investigation of titania–water and alumina–water nanofluids with concentrations from 10^{-5} to 10^{-1} vol.%. They observed CHF to increase with nanoparticle concentration with total enhancements of up to ~115%. Scanning electron micrographs of the heater surface after boiling revealed that it was coated with nanoparticles. Interestingly, when pure water was then boiled on the nanoparticle coated wire, CHF increased up to 2.75 times the baseline, clearly demonstrating that nanofluids increased CHF through surface modification. Furthermore, they demonstrated that nanofluids could actually have a lower CHF than pure fluids given the appropriate surface treatment.

With pure fluids, metallic oxides are known to improve CHF by increasing the wettability of the surface (Tachibana et al., 1967; Liaw and Dhir, 1989; Takata et al., 2005). Tachibana et al. (1967) tested over 400 metallic plates in saturated water pool boiling at atmospheric pressure. They heated the plates to physical destruction and found aluminum to have a much higher CHF due to a native oxide film that developed soon after the initiation of boiling and spread throughout the experiment. Furthermore, stainless steel that was coated with aluminum was found to have a similar enhancement. They believed this higher CHF was due to the oxide's "good affinity" for water. Liaw and Dhir (1989) measured CHF on a vertical copper surface in a saturated water pool at 1 atm. They systematically decreased the static contact angle by heating the copper surface in air to create a thermal oxide. By varying the peak temperature and the amount of time the surface was subjected to heating, the contact angle was decreased from 90° to 14°. CHF was observed to increase by ~90% as the contact angle was decreased.

In summary, the literature to date illustrates an inconsistent effect in the nucleate boiling regime. CHF appears to be enhanced, although the degree of enhancement varies according to research group. The exact mechanisms for the enhancement are not known, and classical theories of CHF provide no explanation. It appears from the existing research that the most probable explanation for CHF enhancement is that the nanofluid alters the surface characteristics of the heater as suggested by numerous researchers. The present study was designed to test whether nanofluid enhancement in CHF is indeed due to its improvement in surface wetting. A water based nanofluid was tested on copper and copper oxide surfaces. Surface wetting was systematically improved by increasing the thermal oxide layer on the copper surface. Ethanol based

nanofluids (with better wetting characteristics) were also used on glass, gold coated, and copper surfaces.

2. Experimental setup and methodology

2.1. Nanofluid preparation

Two concentrated nanofluid suspensions were obtained from Nanophase Technologies Inc.: a 30.84 wt% alumina-in-ethanol suspension, and a 49.5 wt% alumina-in-water suspension. The surface area average diameter and specific surface area of these particles were specified by the manufacturer to be 45 nm and 35 m^2/g, respectively. The nanoparticles were kept in suspension using a proprietary dispersant of unknown concentration (the MSDS list the dispersant concentration as 2–7 wt% and 0.5–20 wt% for water and ethanol based suspensions, respectively).

The ethanol suspension was used as provided by the manufacturer but was diluted to a variety of concentrations between 0.001 and 10.02 g/L. The concentrated suspension was vigorously shaken and then small samples were extracted to be added to pure ethanol. Concentrations were calculated using the following equations:

$$\phi_{Al_2O_3} = 1 - \left(\frac{\rho_{mix} - \rho_{Al_2O_3}}{\rho_{pure\ liquid} - \rho_{Al_2O_3}} \right) \quad (1)$$

$$y_{Al_2O_3} = \frac{\rho_{Al_2O_3}}{\rho_{mix}} \phi_{Al_2O_3} \quad (2)$$

$$c_{Al_2O_3} = \rho_{Al_2O_3} \phi_{Al_2O_3} \quad (3)$$

The water based nanofluids were prepared using a pipette to extract 10 mL from the concentrated suspension. Fluid was drawn from the middle of the concentrated sample to obtain suspended particles rather than those that had coagulated and settled. The solution was weighed to determine the density, ρ_{mix}, of the sample to be used and the volume fraction, mass fraction, and concentration were calculated using Eqs. (1)–(3), respectively. The concentrated water suspension was diluted with distilled water to concentrations from 0.026 to 1.02 g/L.

2.2. Heater design

Two different heaters were used: a thick-film surface mount resistor (Fig. 1) and a solid oxygen free high conductivity (OFHC) copper block (Fig. 2). The 18 Ω ruthenium-based thick-film resistor on an alumina substrate was obtained from Mini-systems Inc. The thick-film heater was supplied with a glass topcoat. The bond pads of the resistor were covered with a layer of silicone to prevent boiling and maintain a uniform boiling surface at the center of the resistor. With only the glass exposed, the surface area was 0.9 cm^2. This heater was subsequently coated with 100 nm of gold through an evaporative physical vapor deposition process. The gold surface decreased the surface energy of the boiling surface, which was done as the first step in the study of surface wettability effects. The average surface temperature was measured with a surface mount, platinum resistance temperature detector (RTD) (Omega Engineering SRTD-2) that was bonded with heatsink compound to the backside of the heater. An aluminum press was used to secure the heater and ensure good thermal contact with the RTD. The entire heater assembly was then glued to a G-10 substrate using electronic grade silicone (GE RTV162). This insulated the backside of the assembly, ensuring negligible temperature difference between the boiling surface and the RTD. Power dissipation was determined by dividing the square of the measured voltage drop across the resistor by the resistance itself.

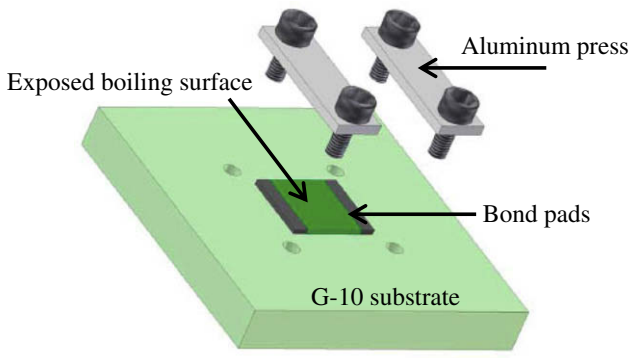

Fig. 1. Thick-film heater assembly (silicone insulation that covered the bond pads is not shown).

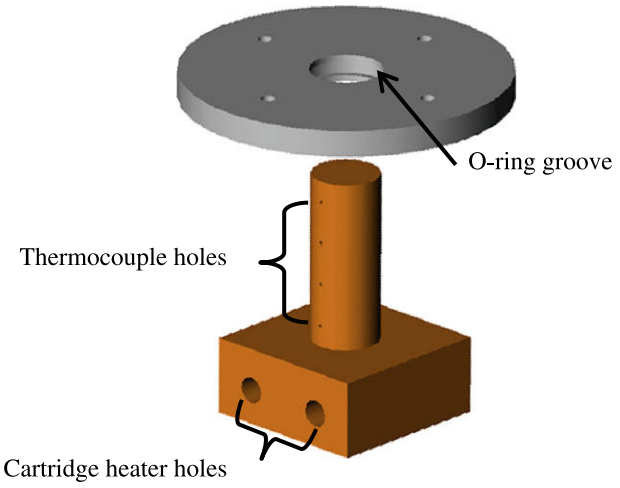

Fig. 2. Copper block heater assembly.

For copper and copper oxide experiments, heat was provided by two 250 W cartridge heaters embedded within an OFHC copper heating block. This block was inserted through a stainless steel plate, which was sealed by two #16 Viton O-rings. The stainless plate was then bolted to the bottom flange of the boiling chamber. The heater block featured a neck with a circular cross-section that terminated with a polished surface on which the boiling occurred. The neck of the heating block contained holes (1 mm diameter, 1 cm deep) for four thermocouples spaced 1 cm apart along its length. The heat flux was calculated assuming 1-D conduction using Fourier's Law based on the temperature gradient in the neck of the copper block. The temperature of the boiling surface was then determined by extrapolating the linear temperature profile out to the wall. The horizontal boiling surface was 2 cm^2 and was polished using emery paper up to 1200 grit, which provided a mirror-like finish. However, a thin region above the O-rings and around the perimeter was also wetted, which increased the total wetted area to 2.7 cm^2. Baseline, unoxidized, polished surfaces were created by using a cotton swab to wipe the surface with dilute nitric acid (1 M HNO_3), which removed the oxidation. Various levels of surface oxidation were then created by heating this copper heating block in air. The use of a single copper heater oxidized to varying degrees instead of multiple heaters enabled us to minimize the effect of surface morphology on the boiling heat transfer.

2.3. Boiling chamber

The stainless steel boiling test rig used in the current study is shown in Fig. 3. The condensing section housed a copper condens-

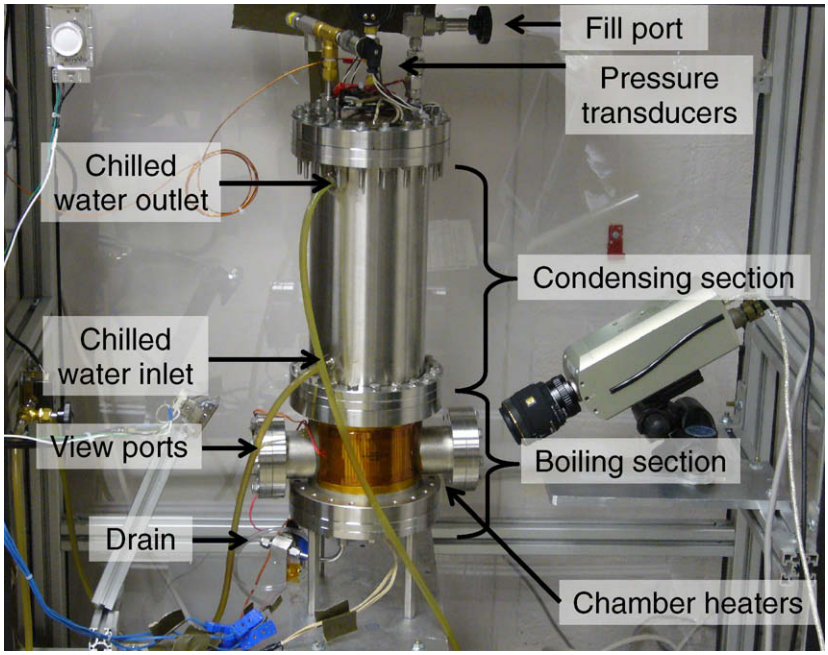

Fig. 3. Photograph of test rig.

ing coil that was cooled by chilled (15±0.2 °C) water provided by a constant temperature bath (NESLAB RTE17). Chamber pressure was measured using a 0–2 atm thin-film pressure transducer (Omega PX212-030AV), and chamber temperature was measured with a Type K thermocouple probe. The chamber temperature was controlled by a proportional-integral-derivative (PID) temperature controller along with Kapton surface heaters that were attached to the outside walls of the lower flange.

The system pressure was reduced prior to each experiment by repeatedly pulling a partial vacuum on the liquid. For the subcooled experiments, dissolved gas (air) remained in the working fluid. In the thick-film heater experiments, the pool temperature was maintained at 30.6 ± 0.5 °C, while the saturation temperature was 51.7 ± 0.4 °C. In the copper block heater experiments, the pool temperature was maintained at 28.8 ± 0.3 °C. These experiments were run at near saturated conditions with a saturation temperature of 29.8 ± 0.7 °C.

2.4. Data acquisition and control

A Fluke Hydra Data Acquisition Unit was used to acquire data from all thermocouples, the flow through the condenser, chamber pressure, RTD resistance, and heater supply voltage. This data was then transferred though a general programming interface bus (GPIB) data link (ICS Electronics 488-USB) to a laptop computer.

Since the small thermal mass (0.4 g) of the thick-film resistor made it highly susceptible to burnout post-CHF, a Wheatstone bridge circuit was used to prevent burnout of the heater by cutting off power. This circuit sensed the balancing of the bridge and output a signal to open two redundant mechanical relays when the heater temperature increased above a set value.

For the copper heating block, cutoff of power to the heaters to prevent burnout was controlled by two redundant on/off temperature controllers with temperature input from the two thermocouples that were closest to the boiling surface.

2.5. Contact angle measurement

Both the advancing and receding contact angle are important during boiling in their effects on the rewetting and bubble growth processes, respectively. The advancing contact angle is much larger than the receding angle, however, and is easier to measure accurately. Since both angles are affected by the liquid's affinity for the solid surface, only the advancing contact angle was measured as an indication of the wettability of the surface.

An advancing contact angle was created by dispensing liquid onto a horizontal surface. A screw driven syringe pump (Harvard Apparatus PHD 2000) was used to infuse liquid onto the surface at a constant rate resulting in a gradually growing liquid droplet. Liquid was delivered at a rate of 125 μL/min through a 305 μm ID microneedle. The measurements were made in an open environment and at room temperature.

A series of digital still photographs were captured by a Nikon D50 with a Sigma 50 mm macro lens. Contact angles were then measured from the digital images using the following algorithm:

(1) Convert the image to grayscale.
(2) Perform edge detection using the Canny (1986) method, which finds local maxima in the gradient of the image.
(3) Choose six points along the droplet/air interface and one on the horizontal heater surface.
(4) Fit an ellipse through the points on the droplet/air interface using the Halif and Flusser (1998) method.
(5) Calculate the tangent at the intersection between this ellipse and the horizontal.
(6) Determine the contact angle from the inverse tangent.

Fig. 4 illustrates the edges of the image detected using the above algorithm, the resulting curve fit, and tangent determination.

3. Uncertainty analysis

The RTD and thermocouples were calibrated with a NIST traceable liquid-in-glass mercury thermometer accurate to within 0.1 °C. To estimate the expected errors, the calibration data was then used in a Monte Carlo simulation with 10,000 iterations. Nominal values plus normally distributed errors were used as inputs to the simulation, and the resultant errors were determined

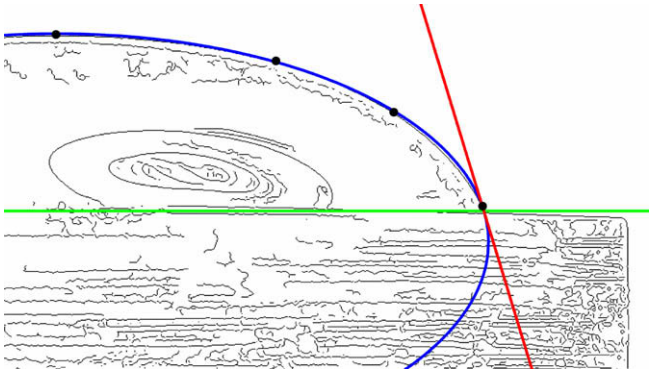

Fig. 4. Example of edge detection using an image of a pure water drop advancing over an unoxidized copper surface.

by finding twice the standard deviation (i.e., 95.5% confidence) of all 10,000 results. The error in the temperature and heat flux dissipated by the thick-film heater was estimated to be 0.1 °C and 4%, respectively. The error in the wall temperature and boiling heat flux with the copper block heater was estimated to be 0.4 °C and 5%, respectively.

4. Results

The first nanofluid tests were performed with ethanol based nanofluids on glass. The boiling curves are shown in Fig. 5. The nanofluid concentration was increased by over two orders of magnitude and no enhancement or degradation in CHF was observed. The nucleate boiling heat transfer coefficient was also not affected by the nanofluid concentration.

Gold was then deposited on the thick-film resistor to decrease the surface energy – the contact angle was still very low, however. The boiling curves for the ethanol based nanofluid on gold are shown in Fig. 6. Effects on CHF enhancement and the nucleate boiling heat transfer coefficient were minimal. The reason for no effect with ethanol based nanofluids is believed to be due to the highly wetting nature of ethanol (see Fig. 7). Most reports in the literature of nanofluid's CHF enhancement concern water based fluids, which is much less wetting than ethanol. If wetting characteristics are

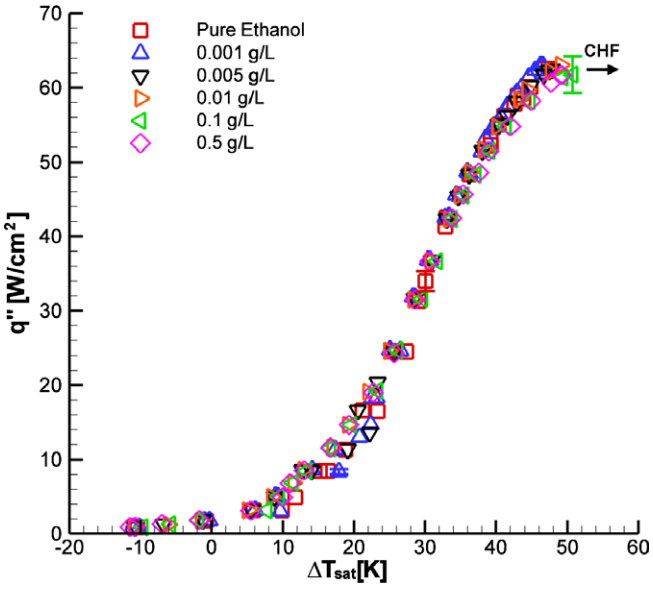

Fig. 5. Boiling curves for alumina/ethanol nanofluid on glass.

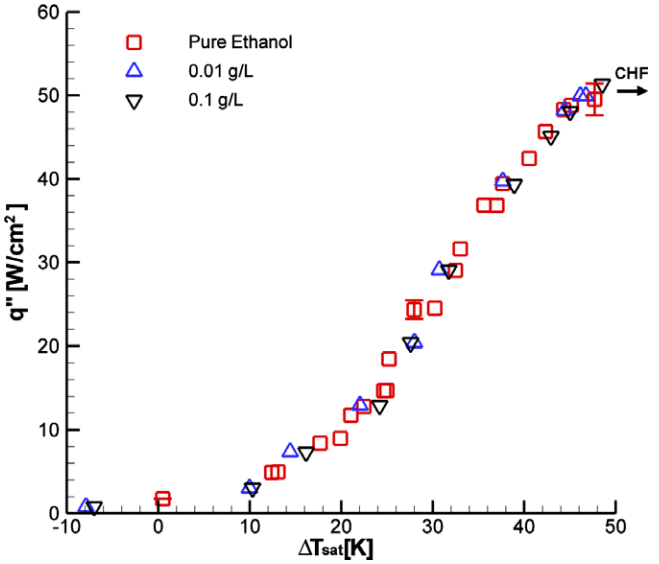

Fig. 6. Boiling curves for alumina/ethanol nanofluid on gold.

important to enhancement as suggested by (Kim et al., 2006b, 2007a), then the CHF of highly wetting base fluids may prove to be more difficult to enhance by the addition of nanoparticles. The relationship between wetting and nanofluid enhancement was therefore systematically investigated by comparing ethanol to water (less wetting) on unoxidized copper (low energy) and oxidized copper (high energy) surfaces.

4.1. Baseline study: pure water on copper and copper oxide

First, the effect of surface wettability on CHF was quantified in the absence of nanofluids. Pure water was tested on a single copper heater oxidized to five different surface oxidation levels. To isolate the effect of the surface oxidation, its wettability was characterized prior to the experiment by measuring the advancing contact angle with pure water. In many cases, the contact angle was also measured after the experiment to determine if further oxidation occurred during the run. The test matrix is shown in Table 1.

As expected, the oxidation reduced the advancing contact angle. There was one anomaly in the contact angle measurements: Trial 6 had an unexplainably large contact angle prior to the experiment. However, its CHF enhancement (discussed below) is in line with expectations given its level of oxidation. Table 1 also shows considerable variation in the contact angle prior to the experiment. This is probably due to the cleaning technique which involved wiping with dilute nitric acid followed by distilled water rinsing, which could quickly produce some oxidation. Despite considerable variation in contact angle prior to the experiments, the unoxidized surfaces had very repeatable CHF. The repeatability with which CHF could be measured on these surfaces may be due to the formation of a native oxide on the surface by the time the CHF data was obtained, as observed by Tachibana et al. (1967). For this reason, the post-CHF contact angle was measured in this study for a number of trials to estimate the contact angle just prior to CHF. The unoxidized surfaces were clearly affected by the boiling process as seen in Table 1.

Boiling curves for pure water that illustrate the effect of surface oxidation are shown in Fig. 8. No effect of oxidation was discernable in the nucleate boiling regime due to scatter in the data. Oxidation, however, tended to increase CHF. The baseline unoxidized surface was run three times with pure water and CHF was repeatedly measured to be 61 ± 1 W/cm^2. The medium/light oxidized sur-

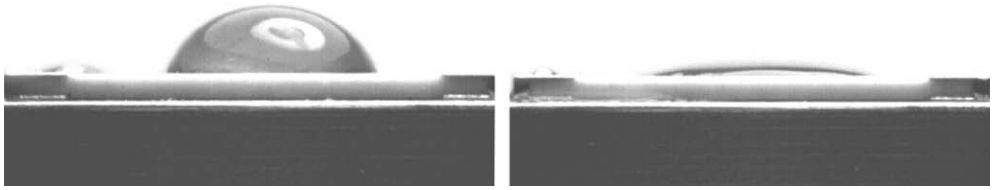

Fig. 7. Photograph of sessile water (left) and ethanol (right) droplets on glass.

Table 1
Test matrix in the order in which it was run

Trial number	Oxidation level	θ_{prior} (°)	θ_{post} (°)
1	None	83 ± 3	63 ± 3
2	None	79 ± 4	64 ± 2
3	Light	56 ± 3	36 ± 4
4	None	65 ± 9	60 ± 4
5	Medium/light	62 ± 8	43 ± 5
6	Medium	97 ± 5	41 ± 4
7	Heavy	25 ± 6	–

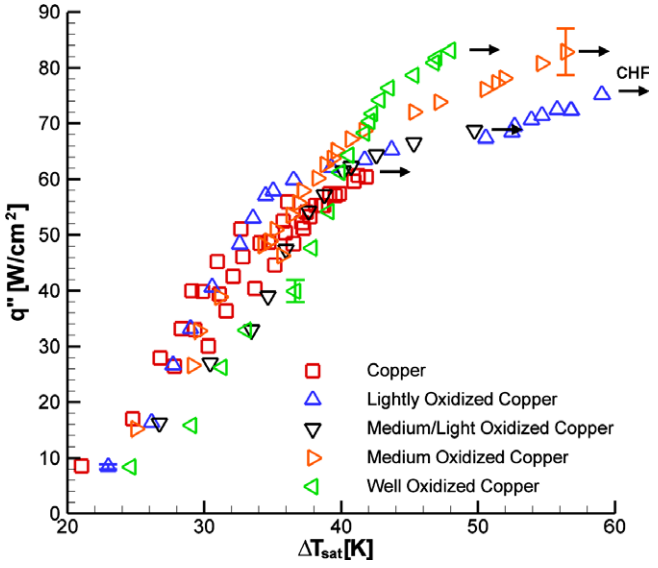

Fig. 8. Boiling curves illustrating the effect of surface oxidation.

face did not have the enhancement one might expect. Noting Table 1, its contact angle was actually higher than the lightly oxidized surface. This information could perhaps have been used to predict its anomalously low CHF. However, the trend is clear: lower contact angle (i.e., oxidation) increases CHF. The well oxidized surface enhanced CHF by 41%, which is in good agreement with the results of Liaw and Dhir (1989) given the contact angle reduction achieved (Fig. 9).

4.2. Alumina/water on copper and copper oxide

Alumina/water nanofluid was then used as the working fluid for the unoxidized copper surface as well as the heavily oxidized copper surface. Boiling curves that illustrate the effect of the nanofluid are shown in Fig. 10. In both cases, nanofluid decreased CHF: by 22% for the oxidized surface and 13% for the unoxidized surface. Initially, these results were unexpected since nanofluids were thought to improve surface wetting (Kim et al., 2006a), which tends to increase CHF. Also note that CHF on the easily wetted copper oxide was degraded more than with the low energy unoxidized

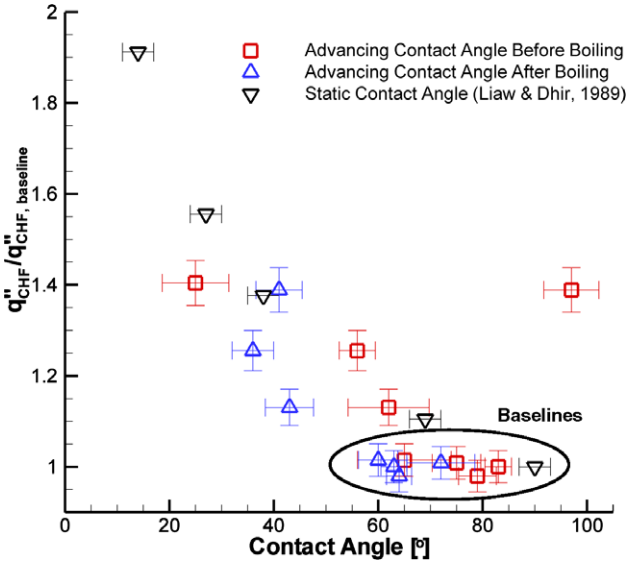

Fig. 9. CHF as a function of contact angle for pure water on copper and copper oxide. Error bars represent standard deviation estimates.

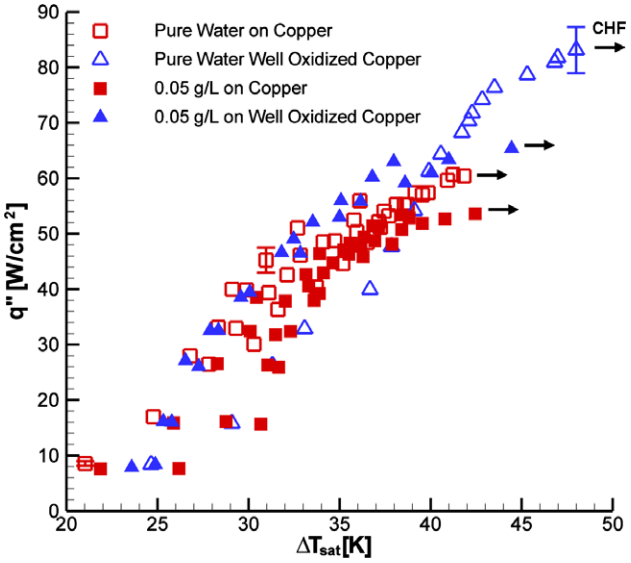

Fig. 10. Boiling curves for dilute alumina/water nanofluid on polished copper and copper oxide.

surface, indicating that an increase in CHF due to improved wettability may be negated by another mechanism such as fouling. Each nanofluid test was immediately repeated, with similar results. The nanofluid was then removed from the chamber, the chamber was thoroughly cleaned and filled with pure water, and a final trial was run. This test yielded a CHF of 62 W/cm^2 compared to the other three baseline CHF measurements of 61 ± 1 W/cm^2, provid-

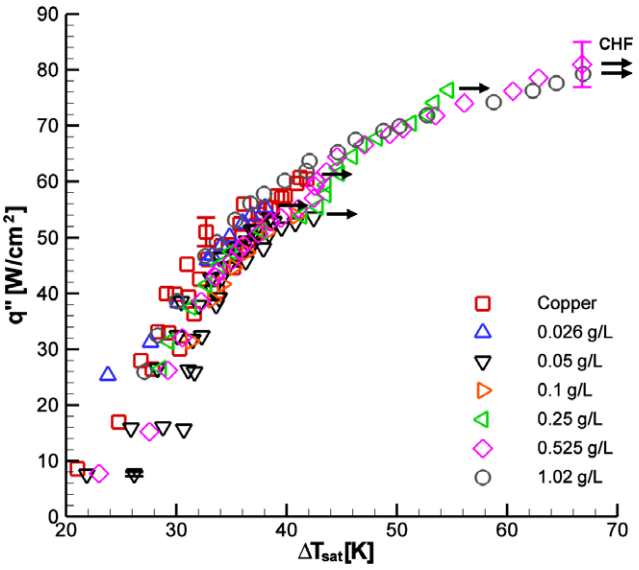

Fig. 11. Boiling curves for alumina/water nanofluids on polished copper.

ing a valuable check on the integrity of the experimental technique and illustrating the consistency of the CHF measurements.

The effect of nanofluid concentration was then determined by using five additional concentrations, increasing the concentration to 20 times the initial value. The nucleate boiling regime was unchanged. However, the boiling curves for an unoxidized surface (Fig. 11) illustrate a significant concentration effect on CHF: dilute

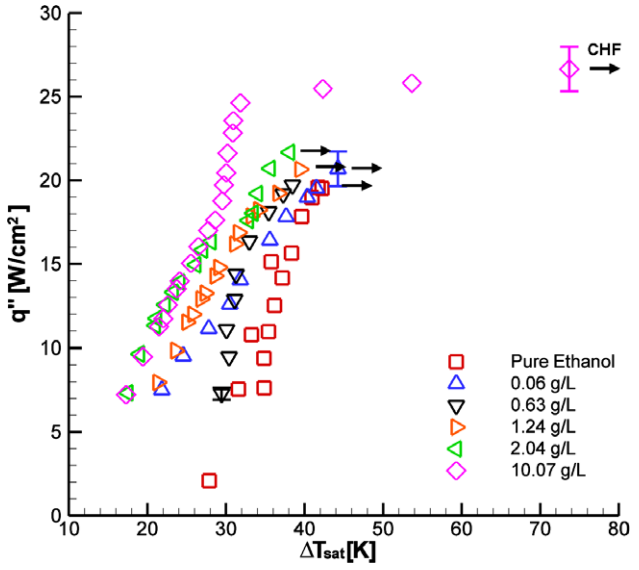

Fig. 12. Boiling curves for alumina/ethanol nanofluids on polished copper.

suspensions caused CHF degradation or had no effect, while higher concentrations increased CHF (up to ~37% with concentrations over 0.525 g/L).

4.3. Alumina/ethanol on pure copper

After observing the strong concentration effect with alumina/water on copper, ethanol based nanofluids were revisited. This time larger concentrations were used with the low energy unoxidized copper surface. The boiling curves (Fig. 12) confirmed that even larger nanoparticle concentrations (10 g/L) were required to enhance CHF with ethanol based nanofluids, and the enhancement was less than with water based nanofluids. Interestingly, the nucleate boiling was improved with increasing nanofluid concentration. The reason(s) for the nucleate boiling enhancement remain unknown. It is possible that the high particle loadings required resulted in a change in nucleation site density. Similarly, it is also possible that the higher relative concentration of proprietary dispersant present in the ethanol based nanofluids may have had a surfactant type effect.

5. Discussion

The results show a strong relationship between boiling performance and the fluid/surface combination. In all cases, nanofluids had a more positive effect when the contact angle was large (surface was more difficult to wet or the base fluid was less wetting). Nanoparticle addition to ethanol had no effect at low concentrations or on easily wetted surfaces. On a copper surface, nanoparticle addition to water provided CHF enhancement of up to ~37% at moderate concentration ($\geqslant$0.525 g/L), but ethanol based fluids required an order of magnitude higher nanoparticle concentration (10 g/L) to obtain a 25% enhancement. Furthermore, when dilute nanofluid was tested on both oxidized and unoxidized copper surfaces, a larger degradation was observed on the more easily wetted oxide surface, demonstrating that the neither the particles alone or the surface/particle interaction can be responsible for the CHF enhancement. Rather, the performance is dependent on the combined effect of particle concentration, surface properties, and the nature of the base fluid.

It is possible that the principal mechanism by which CHF is enhanced with nanofluids is by improving wetting. This model for nanofluid boiling is entirely consistent with the observations above that show that well wetting systems (e.g., ethanol on glass) are unaffected by nanofluid. The ability of nanofluid to enhance wetting was determined by measuring the advancing three-phase contact angle. Photographs of advancing droplets of pure water on copper and 1.02 g/L alumina/water nanofluid on fouled copper are shown in Fig. 13. The nanoparticle fouled copper surface was created by first dispensing nanofluid onto the surface with the infusion pump, then drying the surface with nitrogen gas. The dry-out process left particles on the surface as indicated by the changing contact angle. While the contact angle of pure water was

Fig. 13. Photographs of advancing droplets: water on copper (left) and 1.02 g/L alumina/water nanofluid on nanoparticle fouled copper (right).

89 ± 5°, the nanofluid's contact angle varied according to the degree of fouling. The contact angle of nanofluid on clean surfaces was indistinguishable from pure fluids, but on a fouled surface the contact angle was reduced by 25–50°. Similar experiments were performed with a high energy, oxidized, copper surface. Since the contact angle of pure liquids on high energy surfaces is lower, the effect of the nanofluid was diminished. On an oxidized copper surface, the nanoparticle fouling only resulted in ~10–15° reduction in contact angle. Nanofluid's diminished effect on contact angle on high energy surfaces can plausibly explain why high energy surfaces are not susceptible to nanofluid CHF enhancement.

The current work is consistent with the recent work of Liu and Liao, 2008 who studied pool boiling of nanoparticle suspensions (base fluid + nanoparticles) and nanofluids (base fluid + nanoparticles + surfactant). The mass concentration of nanoparticles was varied from 0.2 wt% to 2 wt%. The CHF for CuO–water nanoparticle suspensions was observed to increase by 27% compared with pure water but the heat transfer was similar in the nucleate boiling regime. For CuO–water nanofluids, strong undulations in the wall temperature were observed when the wall superheat was greater than 12 K and a steady boiling curve could not be obtained. Examination of the surface after the tests indicated the existence of a thin nanoparticle sorption layer on the surface. The surface remained coated with a 500 nm thick layer formed by nanoparticles trapped in the cavities even after removal of the sorption layer with a water jet. The contact angle measured using a sessile drop at room temperature decreased from 45° to 70° on a fresh copper surface to 15–30° after the nanoparticle suspension tests. The CHF increased by about 18% for the SiO_2 nanoparticle suspension compared with pure water, but degradation in the nucleate boiling regime was observed. Similar results were observed with the alcohol based nanofluids and suspensions.

Wen (2008) suggested that nanoparticles on the surface can affect the disjoining pressure at the thin-film interface and shift the triple line towards the vapor (i.e., increase the wettability of the fluid). Changes in the structural disjoining pressure only became significant when the particle concentration increased above 20%, which is likely in the thin-film region since the particles are left in the film as the fluid evaporates.

CHF enhancement due to nanofluids reducing the contact angle might be offset by other detrimental effects such as fouling as noted by Das et al., 2003 and Bang and Chang, 2005. However, if the principal CHF mechanism is improvement of wetting, then surface treatment alone would be preferential to nanofluids. For instance, in the present work, surface oxidation alone produced slightly higher heat transfer than nanofluids but at ~20 °C lower wall superheat.

6. Conclusions

Nanofluids based on two different working fluids were studied in pool boiling on four different surfaces. Performance was found to be highly dependent on both particulate concentration and fluid/surface wetting characteristics. The likely CHF enhancement mechanism for nanofluids appears to be an improvement in the ability of the fluid to wet the surface. Poorly wetting systems could be enhanced by nanofluids (up to ~37%), whereas better wetting systems showed less improvement and required greater nanoparticle concentrations. Moreover, nanofluid combined with nanoparticle fouling was found to improve wetting as determined by a reduction in the advancing three-phase contact angle. Similar CHF enhancement could be achieved using pure fluids on an oxidized surface, however. In fact, surface treatment alone resulted in similar CHF enhancement but at ~20 °C lower wall superheat than required using nanofluids.

Acknowledgments

The authors would like to thank the Office of Naval Research (Dr. Mark Spector was the grant monitor), for their support of this project (Grant No. N000140410315). We would also like to thank Lisa Lucas of the Laboratory for Physical Sciences for assistance with physical vapor deposition. Finally, we would like to acknowledge the assistance of William Michie, Eckhard Lehmann, and Alexander Walzenbach in test rig construction and contact angle measurement.

References

Bang, I.C., Chang, S.H., 2005. Boiling heat transfer performance and phenomena of Al_2–O_3–water nano-fluids from a plain surface in pool boiling. International Journal of Heat and Mass Transfer 48, 2407–2419.

Canny, J., 1986. A computational approach to edge detection. IEEE Transactions on Pattern Analysis and Machine Intelligence 8 (6), 679–698.

Das, S.K., Putra, N., Roetzel, W., 2003. Pool boiling characteristics of nano-fluids. International Journal of Heat and Mass Transfer 46, 851–862.

Halif, R., Flusser, J., 1998. Numerically stable direct least squares fitting of ellipses. In: Proceedings of the Sixth International Conference on Computer Graphics and Visualization, vol. 1, pp. 125–132.

Haramura, Y., Katto, Y., 1983. A new hydrodynamic model of the critical heat flux, applicable widely to both pool and forced convective boiling on submerged bodies in saturated liquids. International Journal of Heat and Mass Transfer 26, 389–399.

Kandlikar, S.G., 2001. A theoretical model to predict pool boiling CHF incorporating effects of contact angle and orientation. Journal of Heat Transfer 123, 1071–1079.

Kim, J.H., Kim, K.H., You, S.M., 2004. Pool boiling heat transfer in saturated nanofluids. In: Proceedings of ASME International Mechanical Engineering Congress and Exposition, November 13–20, 2004, Anaheim, California, Paper No. IMECE2004-61108.

Kim, S.J., Bang, I.C., Buongiorno, J., Hu, L.W., 2006a. Effects of nanoparticle deposition on surface wettability influencing boiling heat transfer in nanofluids. Applied Physics Letters 89, 153107.

Kim, H., Kim, J., Kim, M.H., 2006b. Effect of nanoparticles on CHF enhancement in pool boiling of nano-fluids. International Journal of Heat and Mass Transfer 49, 5070–5074.

Kim, H.D., Kim, J., Kim, M.H., 2007a. Experimental studies on CHF characteristics of nano-fluids at pool boiling. International Journal of Multiphase Flow 33, 691–706.

Kim, S.J., Bang, I.C., Buongiorno, J., Hu, L.W., 2007b. Surface wettability change during pool boiling of nanofluids and its effect on critical heat flux. International Journal of Heat and Mass Transfer 50, 4105–4116.

Liaw, S.P., Dhir, V.K., 1989. Void fraction measurements during saturated pool boiling of water on partially wetted vertical surfaces. Journal of Heat Transfer 111, 731–738.

Liu, Z., Liao, L., 2008. Sorption and agglutination phenomenon of nanofluids on a plain heating surface during pool boiling. International Journal of Heat and Mass Transfer 51, 2593–2602.

Milanova, D., Kumar, R., 2005. Role of ions in pool boiling heat transfer of pure and silica nanofluids. Applied Physics Letters 87, 233107.

Moreno Jr., G., Oldenburg, S.J., You, S.M., Kim, J.H., 2005. Pool boiling heat transfer of alumina-water, zinc oxide-water and alumina–water + ethylene glycol nanofluids. In: Proceedings of HT2005 2005 ASME Summer Heat Transfer Conference, July 17–22, 2005, San Francisco, California, USA.

Narayan, G.P., Anoop, K.B., Das, S.K., 2007. Mechanism of enhancement/deterioration of boiling heat transfer using stable nanoparticle suspensions over vertical tubes. Journal of Applied Physics 102, 074317.

Park, H.S., Shiferaw, D., Sehgal, B.R., Kim, D.K., Muhammed, M., 2004. Film boiling heat transfer on a high temperature sphere in nanofluid. In: Proceedings of ASME HT/FED 2004, vol. 4, pp. 469–476.

Rohsenow, W.M., Griffith, P., 1956. Correlation of Maximum Heat Transfer Data for Boiling of Saturated Liquids. Chemical Engineering Progress Symposium Series 52 (18), 47.

Shi, M.H., Shuai, M.Q., Chen, Z.Q., Li, Q., Xuan, Y., 2007. Study on pool boiling heat transfer of nano-particle suspensions on plate surface. Journal of Enhanced Heat Transfer 14 (3), 223–231.

Tachibana, F., Akiyama, M., Kawamura, H., 1967. Non-hydrodynamic aspects of pool boiling burnout. Journal of Nuclear Science and Technology 4 (3), 121–130.

Takata, Y., Hidaka, S., Cao, J.M., Nakamura, T., Yamamoto, H., Masuda, M., Ito, T., 2005. Effect of surface wettability on boiling and evaporation. Energy 30, 209–220.

Vassalo, P., Kumar, R., D'Amico, S.D., 2004. Pool boiling heat transfer experiments in silica–water nano-fluids. International Journal of Heat and Mass Transfer 47, 407–411.

Wen, D., 2008. Mechanisms of thermal nanofluids on enhanced critical heat flux (CHF). International Journal of Heat and Mass Transfer. doi:10.1016/j.ijheatmasstransfer.2008.01.034.

Wen, D., Ding, Y., 2005. Experimental investigation into the pool boiling heat transfer of aqueous based γ-alumina nanofluids. Journal of Nanoparticle Research 7, 265–274.

Xue, H.S., Fan, J.R., Hu, Y.C., Hong, R.H., Cen, K.F., 2006. The interface effect of carbon nanotube suspension on the thermal performance of a two-phase closed thermosyphon. Journal of Applied Physics 100, 104909.

Yang, Y.M., Maa, J.R., 1984. Boiling of suspension of solid particles in water. International Journal of Heat and Mass Transfer 27 (1), 145–147.

You, S.M., Kim, J.H., Kim, K.H., 2003. Effect of nanoparticles on critical heat flux of water in pool boiling heat transfer. Applied Physics Letters 83 (16), 3374–3376.

Zuber, N., 1959. Hydrodynamic aspects of boiling heat transfer. USAEC Rep. AECU-4439